journal

Theory and Modeling of Glasses and Ceramics

J. Am. Ceram. Soc., **81** [3] 526–32 (1998)

Numerical Simulation of Zener Pinning with Growing Second-Phase Particles

Danan Fan,*,† Long-Qing Chen,*,‡ and Shao-Ping P. Chen†

Theoretical Division, Los Alamos National Laboratory, Los Alamos, New Mexico 87545

Department of Materials Science and Engineering, The Pennsylvania State University, University Park, Pennsylvania 16802

The Zener pinning effect with growing second-phase particles in Al_2O_3–ZrO_2 composite systems were studied by two-dimensional (2-D) computer simulations using a diffuse-interface field model. In these systems, all second-phase particles are distributed at grain corners and boundaries. The second-phase particles grow continuously, and the motion of grain boundaries of the matrix phase is pinned by the second-phase particles which coarsen through the Ostwald ripening mechanism, i.e., long-range diffusion. It is shown that both matrix grains and second-phase particles grow following the power-growth law, $R_t^m - R_0^m = kt$ with $m = 3$. It is found that the mean size of the matrix phase (D) depends linearly on the mean size of the second-phase particles (r) for all volume fractions of second phase from 10% to 40%, which agrees well with experimental results. It is shown that D/r is proportional to the volume fraction of the second phase (f) as $f^{-1/2}$ for a volume fraction less than 30%, which agrees with Hillert and Srolovitz's predictions for 2-D systems, while experimental results from 2-D cross sections of three-dimensional (3-D) Al_2O_3-rich systems showed that either a $f^{-1/2}$ or a $f^{-1/3}$ relation might be possible. It is also found that D/r is not proportional to $f^{-1/3}$ and f^{-1} in 2-D simulations, which suggests that the Zener pinning effect can be very different in 2-D and 3-D systems.

I. Introduction

ZENER pinning is a phenomenon in which second-phase particles retard the coarsening of a matrix phase (grain growth) by pinning the motion of grain boundaries. Since controlling grain size is a critical issue for the processing and application of advanced materials, the inhibition of grain growth by second-phase particles has been extensively studied.[1–6] A detailed theoretical treatment of Zener pinning is very complicated, and a number of approximations have to be introduced.

Zener[1] first derived an analytical model of inhibition of grain growth for three-dimensional (3-D) system by assuming that second-phase particles were spherical, monosized, randomly distributed, and did not coarsen. The grain growth in matrix phase will be stopped and the final grain size is determined by

$$\frac{D}{r} = \frac{4}{3f} \tag{1}$$

where D is the mean grain size of the matrix phase, r is the size of second-phase particles, and f is the volume fraction of second-phase particles. In a more precise calculation, Hellman and Hillert[7] showed that the relation should be $D/r = 8/9f^{-0.93}$ for f less than 0.1. However, they[2,7] indicated that, for a volume fraction f larger than 0.1, the relation should be

$$\frac{D}{r} = \frac{3.6}{f^{1/3}} \tag{2}$$

for 3-D systems when most of the particles are located at grain corners and boundaries. This prediction seems to be supported by the experimental results from different two-phase ceramic systems,[8] in which the pinning relationship for a variety of zirconia- or alumina-based ceramic composites ($f < 0.15$) has been found to be consistent with $1/f^{1/3}$ while the constant for this relation was found to be 0.75 in these systems, smaller than 3.6 in Eq. (2).

Srolovitz *et al.*,[5] on the other hand, showed that in two-dimensional (2-D) systems D/r should be proportional to $1/f$, the same as Eq. (1), if particles are randomly distributed. By assuming that grain growth will stop when there is one particle on each one of the six boundaries of an average grain and all the particles are distributed at grain boundaries, they stated that, in two dimensions,

$$\frac{D}{r} = \frac{3.46}{f^{1/2}} \tag{3}$$

which is different from that for 3-D systems (Eqs. (1) and (2)). Their 2-D Monte Carlo simulations[5] supported this analysis. A similar relation of D/r with $1/f^{1/2}$ was also obtained by Doherty *et al.*[9] for 3-D systems by assuming all particles are in contact with grain boundaries.

The above formulations were obtained by introducing a considerable number of approximations, such as simple geometry (spherical or circle) and monosized particles, and the Q-states Potts model simulations considered only small and immobile second-phase particles which cannot coarsen. While, in real materials, the geometry of particles can be complicated, and if the two phases have limited mutual solubilities, the second-phase particles will grow dynamically as time increases. Therefore, the main purpose of this paper is to examine the relationship between D/r and the volume fraction of a second phase in two-phase systems when the second-phase particles can coarsen.

We employed a diffuse-interface computer simulation model[10–12] for studying the microstructural evolution in two-phase polycrystalline materials. One of the main advantages of this model is that the complexity of microstructural evolution

V. Tikare—contributing editor

Manuscript No. 190984. Received May 16, 1997; approved November 25, 1997.
Presented at the 99th Annual Meeting of The American Ceramic Society, Cincinnati, OH, May 5–7, 1997 (Theory and Computational Modeling Symposium, Paper No. SXIX-024-97).
Supported by the U.S. Department of Energy, Division of Materials Science, Office of Basic Energy Science, and the National Science Foundation under Grant No. DMR 96-33719. The simulations were performed at the Pittsburgh Supercomputing Center and the Advanced Computing Laboratory at the Los Alamos National Laboratory.
*Member, American Ceramic Society.
†Los Alamos National Laboratory.
‡The Pennsylvania State University.

and long-range diffusion in two-phase materials can be automatically taken into account. We employed the well-studied Al_2O_3–ZrO_2 two-phase composite systems as a model system to study the Zener pinning effect, since many thermodynamic and kinetic data are available for these systems.[8,13,14] The detailed computer simulations of microstructural evolution in Al_2O_3–ZrO_2 two-phase composites have been previously reported.[15] We will focus on examining the relationship of the Zener pinning effect on matrix grain size with dynamically growing second-phase particles and comparing simulation results with theoretical analyses.

II. The Diffuse-Interface Field Model

Details about this model have been reported in previous papers,[10–12] and hence only a brief account of the model will be given here. To describe an arbitrary two-phase polycrystalline microstructure, we define a set of continuous field variables[11,12]

$$\eta_1^\alpha(r), \eta_2^\alpha(r), \ldots, \eta_p^\alpha(r), \eta_1^\beta(r), \eta_2^\beta(r), \ldots, \eta_q^\beta(r), C(r) \tag{4}$$

where $\eta_i^\alpha (i = 1, \ldots, p)$ and $\eta_j^\beta (j = 1, \ldots, q)$ are called orientation field variables, with each orientation field representing grains of a given crystallographic orientation of a given phase (denoted as α or β). Those variables change continuously in space and assume continuous values ranging from −1.0 to 1.0. $C(r)$ is the composition field which takes the value of C_α within an α grain and C_β within a β grain.

The total free energy of a two-phase polycrystal system, F, is then written as

$$F = \int \left\{ f_o[C(r);\eta_1^\alpha(r),\eta_2^\alpha(r), \ldots, \eta_p^\alpha(r);\eta_1^\beta(r),\eta_2^\beta(r), \ldots, \eta_q^\beta(r)] + \frac{\kappa_C}{2}[\nabla C(r)]^2 + \sum_{i=1}^{p} \frac{\kappa_i^\alpha}{2}[\nabla \eta_i^\alpha(r)]^2 + \sum_{i=1}^{q} \frac{\kappa_i^\beta}{2}[\nabla \eta_i^\beta(r)]^2 \right\} d^3r \tag{5}$$

where ∇C, $\nabla \eta_i^\alpha$ and $\nabla \eta_j^\beta$ are gradients of concentration and orientation fields, κ_C, κ_i^α, and κ_i^β are the corresponding gradient energy coefficients, f_o is the local free energy density, which is, in this work, assumed to be[11]

$$f_o = f(C) + \sum_{i=1}^{p} f(C,\eta_j^\alpha) + \sum_{i=1}^{q} f(C,\eta_j^\beta) + \sum_{k=\alpha}^{\beta}\sum_{i=1}^{p}\sum_{j=1}^{q} f(\eta_i^k,\eta_j^k) \tag{6}$$

in which

$$f(C) = -(A/2)(C - C_m)^2 + (B/4)(C - C_m)^4 + (D_\alpha/4)(C - C_\alpha)^4 + (D_\beta/4)(C - C_\beta)^4$$

$$f(C,\eta_j^\alpha) = -(\gamma_\alpha/2)(C - C_\beta)^2(\eta_i^\alpha)^2 + (\delta_\alpha/4)(\eta_i^\alpha)^4$$

$$f(C,\eta_j^\beta) = -(\gamma_\beta/2)(C - C_\alpha)^2(\eta_i^\beta)^2 + (\delta_\beta/4)(\eta_i^\beta)^4$$

$$f(\eta_i^k,\eta_j^k) = (\varepsilon_{ij}^{kk}/2)(\eta_i^k)^2(\eta_j^k)^2$$

where C_α and C_β are the equilibrium compositions of α and β phases, $C_m = (C_\alpha + C_\beta)/2$, A, B, D_α, D_β, γ_α, γ_β, δ_α, δ_β, and ε_{ij}^{kk} are phenomenological parameters. The justification of using such a free-energy model in the study of coarsening was previously discussed.[11]

The temporal evolution of the field variables are described by the time-dependent Ginzburg–Landau (TDGL)[16] and Cahn-Hilliard[17] equations.

$$\frac{d\eta_i^\alpha(r,t)}{dt} = -L_i^\alpha \frac{\delta F}{\delta \eta_i^\alpha(r,t)} \qquad i = 1, 2, \ldots, p \tag{7a}$$

$$\frac{d\eta_i^\beta(r,t)}{dt} = -L_i^\beta \frac{\delta F}{\delta \eta_i^\beta(r,t)} \qquad i = 1, 2, \ldots, q \tag{7b}$$

$$\frac{dC(r,t)}{dt} = \nabla\left\{ L_C \nabla\left[\frac{\delta F}{\delta C(r,t)} \right] \right\} \tag{7c}$$

where L_i^α, L_i^β and L_C are kinetic coefficients related to grain boundary mobilities and atomic diffusion coefficients, t is time, and F is the total free energy given in Eq. (5).

III. Numerical Methodology

The microstructural evolution of a two-phase system can be simulated by solving coupled kinetic Eq. (7). To numerically solve the set of kinetic equations, one needs to discretize them with respect to space. We discretize the Laplacian using the following approximation:

$$\nabla^2\phi = \frac{1}{(\Delta x)^2}\left[\frac{1}{2}\sum_j (\phi_j - \phi_i) + \frac{1}{4}\sum_{j'} (\phi_{j'} - \phi_i) \right] \tag{8}$$

where ϕ is any function, Δx is the grid size, j represents the set of first nearest neighbors of i, and j' is the set of second nearest neighbors of i. For discretization with respect to time, we employed the following simple Euler technique:

$$\phi(t + \Delta t) = \phi(t) + \frac{d\phi}{dt} \times \Delta t \tag{9}$$

where Δt is the time step for integration. All the results discussed below were obtained by using $\Delta x = 2.0$, $\Delta t = 0.1$ to ensure the numerical stability. The kinetic equations are discretized using 512 × 512 points with periodic boundary conditions applied along both directions. The total number of orientation field variables for two phases is 30.

In the Al_2O_3–ZrO_2 systems, it was reported[8,18] that the ratio of the grain boundary energy to the interphase energy for the Al_2O_3 phase (denoted as α phase) is $R_\alpha = \sigma_{alu}^\alpha/\sigma_{int}^{\alpha\beta} = 1.4$, and that for the ZrO_2 phase (denoted as β phase) is $R_\beta = \sigma_{zir}^\beta/\sigma_{int}^{\alpha\beta} = 0.97$. We assumed isotropic grain boundary and interphase boundary energies. It is found that parameters $A = 2.0$, $B = 9.88$, $C_\alpha = 0.01$, $C_\beta = 0.99$, $D_\alpha = D_\beta = 1.52$, $\gamma_\alpha = \gamma_\beta = 1.23$, $\delta_\alpha = \delta_\beta = 1.0$, $\varepsilon = 7.0$, $\kappa_C = 1.5$, $\kappa_i^\alpha = 2.5$ and $\kappa_i^\beta = 2.0$ give the correct grain boundary to interphase boundary energy ratios for the Al_2O_3–ZrO_2 system.[11] We also assumed that both phases have the same diffusivity and grain boundary mobility.

All the kinetic data and size distributions were obtained using 512 × 512 grid points and averaged from three independent runs. There are more than 2700 grains at the beginning of collecting data for calculating the statistics and there are about 200 at the end. To generate the initial two-phase microstructure, a single-phase grain growth simulation was first performed to obtain a fine-grain structure. Grains are then randomly assigned with the equilibrium composition C_α or C_β and an orientation field, keeping the overall average composition corresponding to the desired equilibrium volume fractions. The grain area was measured by counting all points within a grain, and the grain size R was calculated by assuming area $A = \pi R^2$.

IV. Simulation Results and Discussion

The details of kinetics and microstructural evolution in ZrO_2–Al_2O_3 two-phase composites have been previously discussed.[11,13] Six representative simulated two-phase microstructures at six different volume fractions of the ZrO_2 phase are shown in Fig. 1. In these microstructures, ZrO_2 grains are bright and Al_2O_3 grains are gray. It can be seen that simulated microstructures have a striking resemblance to those of experimental observations.[18] All the main features of coupled grain growth and Ostwald ripening, observed experimentally, are predicted by the computer simulations. For example, at a low

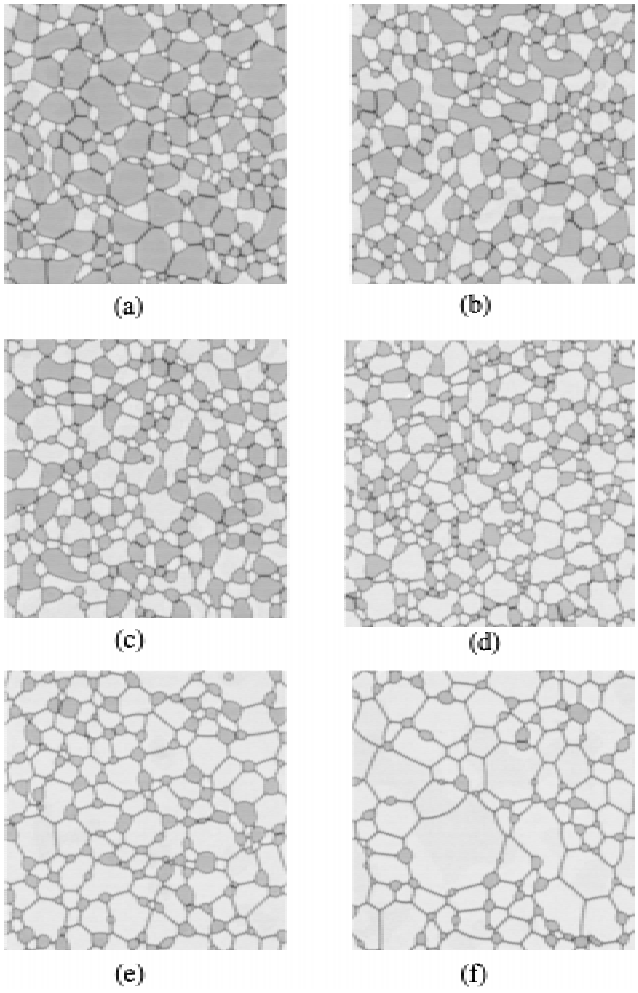

Fig. 1. Typical simulated microstructures in Al_2O_3–ZrO_2 systems with different volume fractions of ZrO_2 phase: (a) 30%; (b) 50%; (c) 60%; (d) 70%; (e) 80%; (f) 90%. System size is 512 × 512. ZrO_2 grains are bright and Al_2O_3 grains are gray.

volume fraction of ZrO_2 phase, the particles of ZrO_2 phase are located mainly at trijunctions and grain boundaries of Al_2O_3 grains, and the coarsening of these particles is controlled by the Ostwald ripening process; i.e., relatively large particles grow at the expense of smaller ones by long-range diffusion. The motion of grain boundaries of Al_2O_3 grains is essentially pinned by the ZrO_2 particles, and the grain size of Al_2O_3 grains is fixed by the locations and distributions of ZrO_2 particles. During microstructural evolution or coarsening, all second-phase particles are in contact with grain boundaries.

The time dependencies of the average grain size in the 10% ZrO_2 system with the initial microstructure generated from a fine-grain structure are shown in Fig. 2 for Al_2O_3 (α-phase) and in Fig. 3 for ZrO_2 (β-phase). In these plots, the dotted lines are the data measured from the simulated microstructures, and the solid lines are the nonlinear fits to the power growth law $R_t^m - R_o^m = kt$. It can be seen that both second-phase particles and matrix grain size grow dynamically as time increases. According to the nonlinear fits, growth kinetics for both matrix phase and second phase particles follow the power law with $m = 3$, a strong indication that the coarsening kinetics are controlled by the long-range diffusion. The kinetic coefficient k for the α phase is 31.85, and is 0.785 for the β-phase in the 10% β-phase system, which is about 1/50 that for the α-phase. This dramatic variation comes from the different diffusion distances of the two phases during coarsening as the volume fraction changes. For the low volume fraction β-phase, the coarsening kinetics are controlled solely by Ostwald ripening and

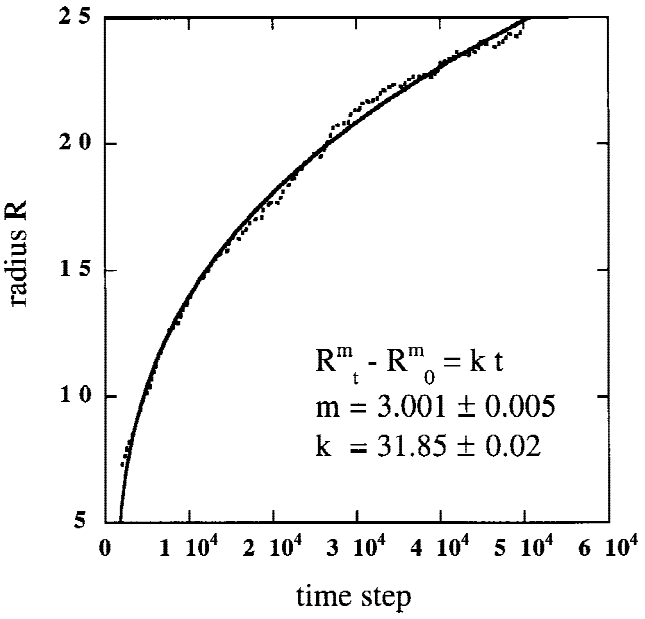

Fig. 2. Time dependence of the average grain size of Al_2O_3 (α) phase. The volume fraction of ZrO_2 phase is 10%. $R_\alpha = 1.4$, $R_\beta = 0.97$. The dots are the measured data from simulated microstructures. The solid line is a nonlinear fit to the power growth law $R_t^m - R_0^m = kt$ with three variables m, k, and R_0.

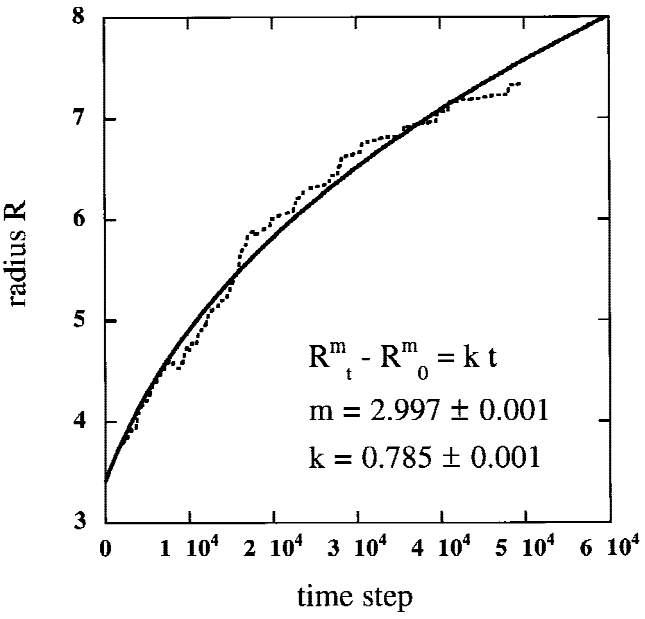

Fig. 3. Time dependence of the average grain size of ZrO_2 (β) phase. The volume fraction of ZrO_2 phase is 10%. $R_\alpha = 1.4$, $R_\beta = 0.97$. The dots are the measured data from simulated microstructures. The solid line is a nonlinear fit to the power growth law $R_t^m - R_0^m = kt$ with three variables m, k, and R_0.

the typical diffusion distance is about the typical separation distance between β-phase grains. However, grain growth for the high volume fraction of α-phase depends on the fraction of grain boundaries that are pinned by β grains, and therefore the volume fraction of β. It has been shown that the variation of volume fractions will dramatically change the coarsening kinetics of both phases.[11,15]

Experimentally, Alexander *et al.*[19] have examined the relationship between the matrix grain size and the size of growing second-phase particles in alumina-rich, zirconia-toughened

composites. They showed that a good linear relationship between the average alumina grain size (D) with the mean zirconia particle size (r) is maintained at all zirconia contents (10% ~ 40%), as shown in Fig. 4. The ratio of the alumina/zirconia grain size (D/r) is constant at a given volume fraction of zirconia phase,[19] which does not change with sintering time and temperature. They found that the ratio D/r decreases with increasing volume fraction of the zirconia phase, and the ratios observed are 4.6, 3.5, and 2.1 for 10%, 20%, and 40% of zirconia phase,[19] respectively. The relationship of D/r with growing zirconia particles, from computer simulations, is shown in Fig. 5, for alumina–zirconia composites with 10%, 20%, and 40% of zirconia. It can be seen that all features observed experimentally have been predicted from computer simulations. It is clear that a good linear relationship exists between D and r at all zirconia volume fractions, and the ratio D/r decreases as the volume fraction of zirconia increases. From computer simulations, the ratios D/r are predicted as 4.4, 3.1 and 1.6, for 10%, 20%, and 40% of zirconia, respectively. The agreement between computer simulations and experimental results is surprisingly good, considering the assumptions we made in the simulations and the fact that we only fitted the data of grain boundary energies and interfacial energy.

To compare the simulation results with analytical solutions (Eqs. (1)–(3)), we plot the matrix grain size (D) against the size (r) of second-phase particles, which is normalized by an appropriate form of volume fraction. For example, to examine if D/r has a relationship with volume fraction as $1/f^{1/3}$, we plot D against $r/f^{1/3}$ for different volume fractions. It is obvious that if that relation is obeyed, a common slope (or constant A) should be found for different volume fractions of second phase, which satisfies the equation $D = Ar/f^{1/3}$. Figures 6 and 7 show the simulation results for the relationships of matrix grain size D with second-phase particle size r normalized with $1/f^{1/3}$ for the Al_2O_3-rich and the ZrO_2-rich systems, respectively. In these plots, the volume fraction of second phase (ZrO_2 or Al_2O_3) varies from 10% to 40%. It can be seen that the slopes of these linear relations at different volume fractions are different for both Al_2O_3-rich and ZrO_2-rich two-phase systems, indicating that there is no unique A which can be found to satisfy the relation $D = Ar/f^{1/3}$ for different volume fractions. This suggests that D/r is not proportional to $1/f^{1/3}$ in these 2-D two-phase systems. However, experimental results[8] showed that the relation $D = Ar/f^{1/3}$ is followed in zirconia- or alumina-based ceramic composites with $f < 0.15$. Hence, the relation $D = Ar/f^{1/3}$ may apply only to 3-D systems.

The relation $D = Ar/f$ is examined from simulations for Al_2O_3-rich systems and ZrO_2-rich systems in Figs. 8 and 9, respectively. It is clear that this relation is not obeyed in small volume fraction systems. However, it is interesting to notice that in high volume fraction systems (30% and 40% second phase) a fairly good relation might be found for both Al_2O_3-rich and ZrO_2-rich systems. The relation $D = Ar/f$ for 3-D systems (Eq. (1)) was obtained by assuming the numbers of

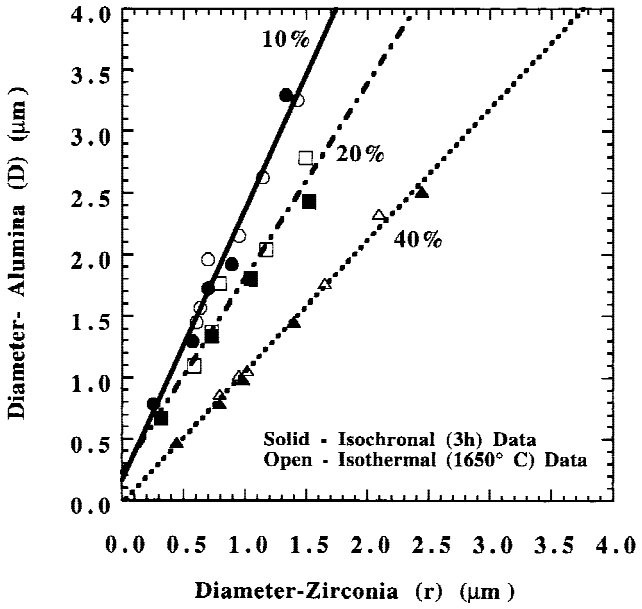

Fig. 4. Experimental results for the dependence of mean diameters (D) of alumina phase on mean diameters (r) of zirconia phase after isochronal and isothermal treatments at different volume fractions of zirconia. (Experimental data are adapted from Fig. 5 of Ref. 22, by Alexander *et al.*) The D/r ratios are 4.6, 3.5, and 2.1 for 10%, 20%, and 40% of zirconia phase, respectively.

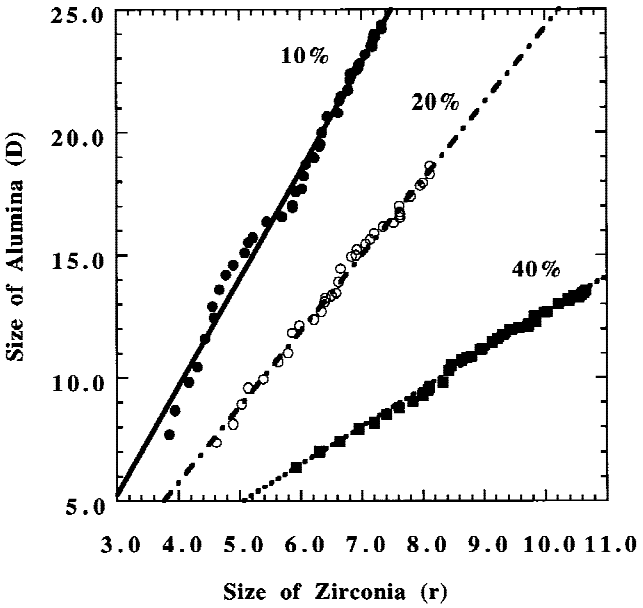

Fig. 5. Simulation results for the dependence of mean size (D) of alumina phase on mean size (r) of zirconia phase as a function of zirconia volume fraction. The D/r ratios are 4.4, 3.1, and 1.6 for 10%, 20%, and 40% of zirconia phase, respectively.

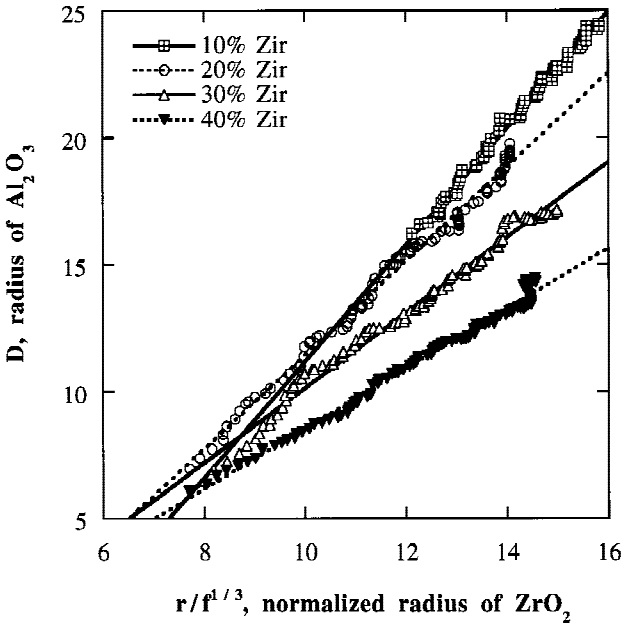

Fig. 6. Simulation results for the relations of matrix grain size D with the second-phase particle size r normalized with $1/f^{1/3}$ for Al_2O_3–ZrO_2 two-phase systems. The Al_2O_3 phase is the matrix phase.

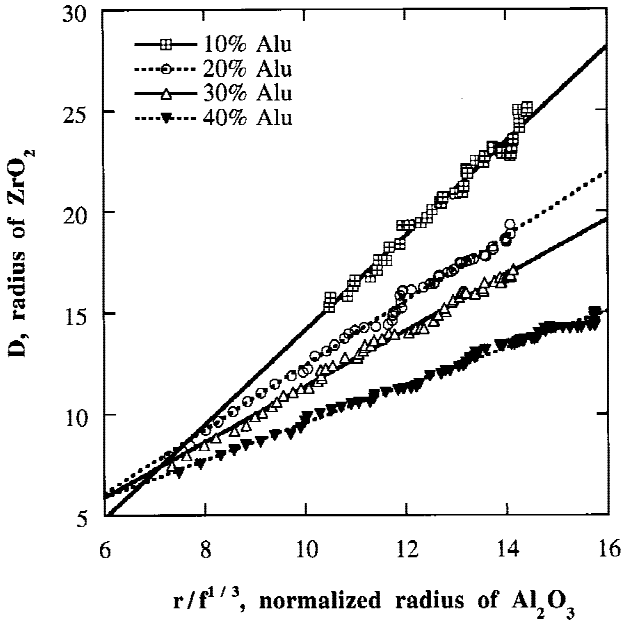

Fig. 7. Simulation results for the relations of matrix grain size D with the second-phase particle size r normalized with $1/f^{1/3}$ for Al_2O_3–ZrO_2 two-phase systems. The ZrO_2 phase is the matrix phase.

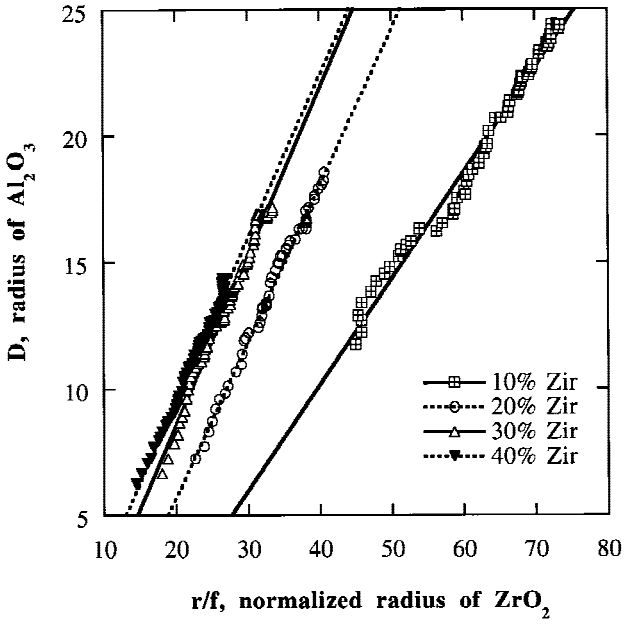

Fig. 8. Simulation results for the relations of the matrix grain size D with the second-phase particle size r normalized with $1/f$ for Al_2O_3–ZrO_2 two-phase systems. The Al_2O_3 phase is the matrix phase.

particles at a boundary proportional to the particle radius and a random particle distribution. However, this is not the case in these simulations of high volume fraction systems, in which all second-phase grains stay at grain boundaries and become interpenetrated at 40%. Liu and Patterson[20,21] modified the Zener's equation in 2-D by accounting for the nonrandomness of the particle distribution. By defining a parameter $R = f_{gb}/f$, the degree of contact between grain boundaries and second-phase particles, where f_{gb} is the area fraction of second phase at the grain boundaries and f the total fraction, they obtained $D/r = \pi/4Rf$. The R value, which varies among material systems, and with volume fraction, particle size, etc.,[20,21] was not calculated in current simulations. Therefore, whether 2-D Al_2O_3–ZrO_2 systems follow this equation remains to be more carefully examined.

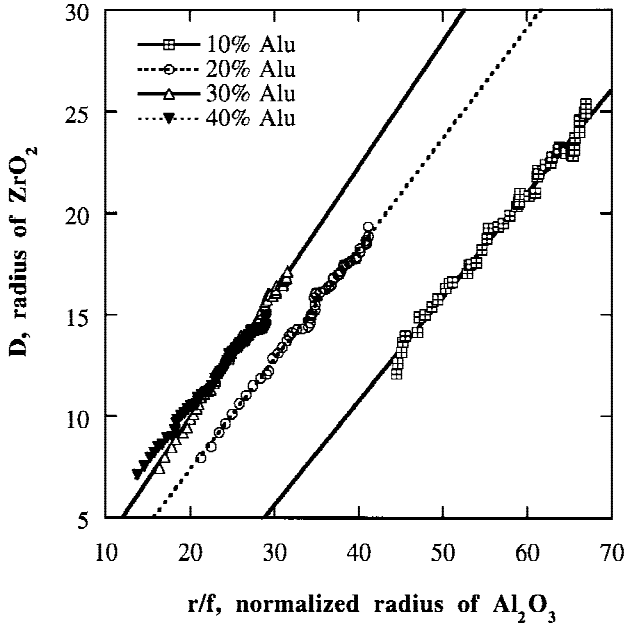

Fig. 9. Simulation results for the relations of the matrix grain size D with the second-phase particle size r normalized with $1/f$ for Al_2O_3–ZrO_2 two-phase systems. The ZrO_2 phase is the matrix phase.

Figures 10 and 11 show the simulated relations of the matrix grain size D with $r/f^{1/2}$ in Al_2O_3-rich and ZrO_2-rich two-phase systems. It is found that the relation $D = Ar/f^{1/2}$ is followed reasonably well for volume fractions of second phases equal or less than 30%, with the constant A values being 1.32 for Al_2O_3-rich systems and 1.27 for ZrO_2-rich systems. These A values are much smaller than 3.4, which was obtained by Srolovitz *et al.*[5] for small and immobile particles. The smaller A values mean a smaller matrix grain size at a certain size of second-phase particles. Therefore, the pinning effect of growing second-phase particles is much stronger than that in systems with

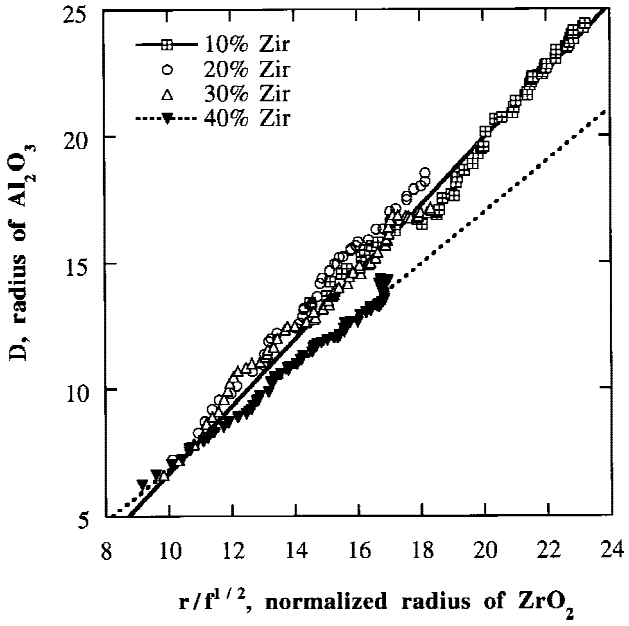

Fig. 10. Simulation results for the relations of the matrix grain size D with the second-phase particle size r normalized with $1/f^{1/2}$ for Al_2O_3–ZrO_2 two-phase systems. The Al_2O_3 phase is the matrix phase.

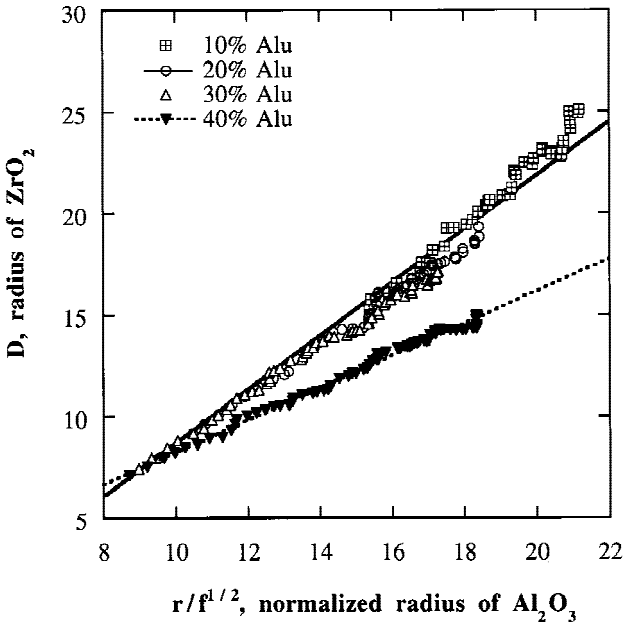

Fig. 11. Simulation results for the relations of the matrix grain size D with the second-phase particle size r normalized with $1/f^{1/2}$ for Al_2O_3–ZrO_2 two-phase systems. The ZrO_2 phase is the matrix phase.

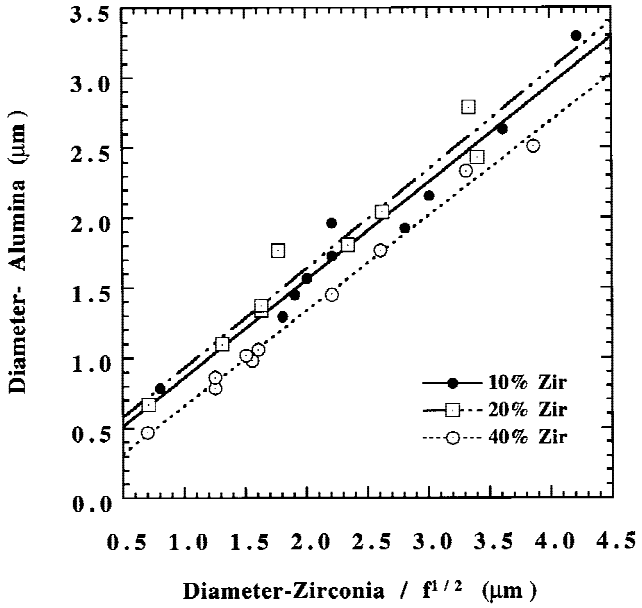

Fig. 12. Experimental observations of the relation of the mean diameters of alumina with mean diameters of zirconia normalized with $1/f^{1/2}$. (Experimental data are adapted from Fig. 5 of Ref. 19, by Alexander *et al.*)

small and noncoarsening particles. The main reason for the larger pinning effect in the studied composite systems is that it is almost impossible for grain boundaries to pass through second-phase particles in these long-range diffusion-controlled systems. It is also interesting to notice that the difference of grain boundary energies in alumina and zirconia does not affect the relationship of Zener pinning in these simulations. Even though the coarsening rate for alumina and zirconia matrix can be slightly different, both Al_2O_3-rich and ZrO_2-rich two-phase systems show identical relationships of Zener pinning in these simulations. When the volume fraction of second phase is larger than 40%, the relation $D = Ar/f^{1/2}$ is not followed anymore, which may result from the fact that at this volume fraction the second-phase grains become interconnected in a two-phase microstructure.

To compare the 2-D simulation results with experimental observations, we re-plot the experimental data (Fig. 4, adapted from Ref. (19)) with the normalized second-phase (zirconia) grain size in Figs. 12, 13, and 14. It should be noted that these experimental data were obtained from the 2-D cross sections of 3-D microstructures,[19] which may be different from 2-D systems. It is quite clear that the relation $D = Ar/f$ is not followed by those experimental systems either. While there may not be enough evidence to conclude that the relation $D = Ar/f^{1/3}$ is not obeyed in those systems ($f < 10\%$), it is obvious that $D = Ar/f^{1/2}$ fits these experimental data better for volume fractions between 10% and 20%. Since most of the second-phase grains are distributed at grain boundaries[19] in these two-phase composites, it seems that those experimental results agree with the analysis by Doherty *et al.*[9] for 3-D systems, in which a $D = Ar/f^{1/2}$ relation is predicted by assuming all particles are in contact with grain boundaries. As mentioned before, in zirconia- or alumina-based ceramic composites, a $D = Ar/f^{1/3}$ relation was observed[8] for $f < 0.15$. Therefore, it can be seen that Zener pinning effect may depend on the dimensionality, volume fraction, and distribution of second-phase particles.

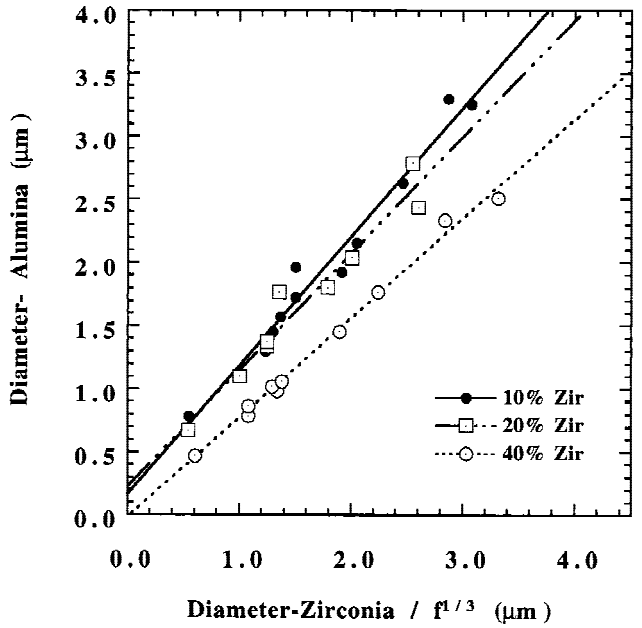

Fig. 13. Experimental observations of the relation of the mean diameters of alumina with mean diameters of zirconia normalized with $1/f^{1/3}$. (Experimental data are adapted from Fig. 5 of Ref. 19, by Alexander *et al.*)

V. Conclusions

The Zener pinning effect with growing second-phase particles in the Al_2O_3–ZrO_2 two-phase composites has been studied through computer simulations using a diffuse-interface field model. The simulated microstructures are in excellent qualitative agreement with experimental observations for Al_2O_3–ZrO_2 two-phase composites. It is found that the coarsening kinetics for both phases are controlled by long-range diffusion and follow the power growth law $R_t^m - R_o^m = kt$ with $m = 3$, while the kinetic coefficient k for the second-phase particles is much smaller than that of the matrix phase. A linear relation between matrix grain size (D) and second-phase grain size (r) is found for all volume fractions of second phase, which agrees with experimental results. The D/r ratios are dependent on the volume fraction of the second phase and are predicted as 4.4, 3.1, and 1.6 for 10%, 20%, and 40% of zir-

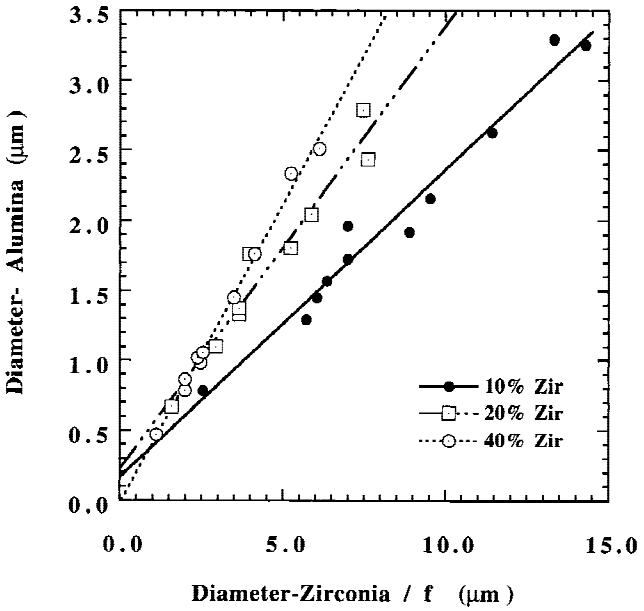

Fig. 14. Experimental observations of the relation of the mean diameters of alumina with mean diameters of zirconia normalized with 1/*f*. (Experimental data are adapted from Fig. 5 of Ref. 19, by Alexander *et al.*)

conia, respectively, which are very close to experimental observations. It is found that the relationship between matrix grain size and second-phase grain size follows $D = Ar/f^{1/2}$ in the 2-D simulations when the volume fraction of the second phase is less than 30%. The $1/f^{1/3}$ and $1/f$ relationships are not observed in these 2-D two-phase simulation systems with dynamically growing second-phase particles. Comparison with experimental results shows that the Zener pinning effect may depend on the dimensionality, volume fraction, and distribution characteristics of the second-phase particles.

References

[1]C. Zener, quoted by C. S. Smith, ''Grains, Phases, and Interfaces: An Interpretation of Microstructure,'' *Trans. AIME*, **175**, 15 (1948).

[2]M. Hillert, ''Inhibition of Grain Growth by Second-Phase Particles,'' *Acta Metall.*, **36**, 3177 (1988).

[3]G. Grewal and S. Ankem, ''Modeling Matrix Grain Growth in the Presence of Growing Second Phase Particles in Two Phase Alloys,'' *Acta Metall. Mater.*, **38**, 1607 (1990).

[4]J. D. French, M. P. Harmer, H. M. Chan, and G. A. Miller, ''Coarsening-Resistant Dual-Phase Interpenetrating Microstructures,'' *J. Am. Ceram. Soc.*, **73**, 2508 (1990).

[5]D. J. Srolovitz, M. P. Anderson, G. S. Grest, and P. S. Sahni, ''Computer Simulation of Grain Growth—III. Influence of a Particle Dispersion,'' *Acta Metall.*, **32**, 1429 (1984).

[6]G. N. Hassold, E. A. Holm, and D. J. Srolovitz, ''Effects of Particle Size on Inhibited Grain Growth,'' *Scr. Metall.*, **24**, 101 (1990).

[7]P. Hellman and M. Hillert, ''On the Effect of Second-Phase Particles on Grain Growth,'' *Scand. J. Met.*, **4**, 211 (1975).

[8]I-Wei Chen and L. A. Xue, ''Development of Superplastic Structural Ceramics,'' *J. Am. Ceram. Soc.*, **73**, 2585 (1990) and references therein.

[9]R. D. Doherty, D. J. Srolovitz, A. D. Rollett, and M. P. Anderson, ''On the Volume Fraction Dependence of Particle Limited Grain Growth,'' *Scr. Metall.*, **21**, 675 (1987).

[10]L.-Q. Chen and D. Fan, ''Computer Simulation Model for Coupled Grain Growth and Ostwald Ripening—Application to Al_2O_3–ZrO_2 Two-Phase Systems,'' *J. Am. Ceram. Soc.*, **79**, 1163 (1996).

[11]D. Fan and L.-Q. Chen, ''Diffusion-Controlled Grain Growth in Two-Phase Solids,'' *Acta Mater.*, **45** [8] 3297–310 (1997).

[12]D. Fan and L.-Q. Chen, ''Topological Evolution during Coupled Grain Growth and Ostwald Ripening in Volume-Conserved 2-D Two-Phase Polycrystals,'' *Acta Mater.*, **45** [10] 4145–54 (1997).

[13]M. P. Harmer, H. M. Chen, and G. A. Miller, ''Unique Opportunities for Microstructural Engineering with Duplex and Laminar Ceramic Composite,'' *J. Am. Ceram. Soc.*, **75**, 1715 (1992).

[14]K. B. Alexander, ''Grain Growth and Microstructural Evolution in Two-Phase Systems: Alumina/Zirconia Composites,'' Short Course on ''Sintering of Ceramics'' at the American Ceramic Society Annual Meeting, Cincinnati, OH, April 1995.

[15]D. Fan and L.-Q. Chen, ''Computer Simulation of Grain Growth and Ostwald Ripening in Alumina–Zirconia Two-phase Composites,'' *J. Am. Ceram. Soc.*, **80** [7] 1773–80 (1997).

[16]S. M. Allen and J. W. Cahn, ''A Microscopic Theory for Antiphase Domain Boundary Motion and Its Application to Antiphase Domain Coarsening,'' *Acta Metall.*, **27**, 1085 (1979).

[17]J. W. Cahn, ''On Spinodal Decomposition,'' *Acta Metall.*, **9**, 795–801 (1961).

[18]G. Lee and I-W. Chen, ''Sintering and Grain Growth in Tetragonal and Cubic Zirconia''; Vol. 1, pp. 340–46 in Sintering '87, Proceedings of the 4th International Symposium on Science and Technology of Sintering (Tokyo, Japan, 1987). Edited by S. Somiya, M. Shimada, M. Yoshimura, and R. Watanabe. Elsevier Applied Science, London, U.K., 1988.

[19]K. B. Alexander, P. B. Becher, S. B. Waters, and A. Bleier, ''Grain Growth Kinetics in Alumina–Zirconia (CeZTA) Composites,'' *J. Am. Ceram. Soc.*, **77** [4] 939 (1994).

[20]Y. Liu and B. R. Patterson, ''Stereological Analysis of Zener Pinning,'' *Acta Metall. Mater.*, **44**, 4327 (1996).

[21]Y. Liu and B. R. Patterson, ''A Stereological Model of the Degree of Grain Boundary—Pore Contact during Sintering,'' *Metall. Trans. A*, **24**, 1497 (1993).

□